



**HAL**  
open science

# Pyrolysis of biomass in a batch fluidized bed reactor: Effect of the pyrolysis conditions and the nature of the biomass on the physicochemical properties and the reactivity of char

Mathieu Morin, Sébastien Pécate, Mehrdji Hemati, Yilmaz Kara

## ► To cite this version:

Mathieu Morin, Sébastien Pécate, Mehrdji Hemati, Yilmaz Kara. Pyrolysis of biomass in a batch fluidized bed reactor: Effect of the pyrolysis conditions and the nature of the biomass on the physicochemical properties and the reactivity of char. *Journal of Analytical and Applied Pyrolysis*, 2016, 122, pp.511-523. 10.1016/j.jaap.2016.10.002 . hal-01907322

**HAL Id: hal-01907322**

**<https://hal.science/hal-01907322>**

Submitted on 29 Oct 2018

**HAL** is a multi-disciplinary open access archive for the deposit and dissemination of scientific research documents, whether they are published or not. The documents may come from teaching and research institutions in France or abroad, or from public or private research centers.

L'archive ouverte pluridisciplinaire **HAL**, est destinée au dépôt et à la diffusion de documents scientifiques de niveau recherche, publiés ou non, émanant des établissements d'enseignement et de recherche français ou étrangers, des laboratoires publics ou privés.



## Open Archive Toulouse Archive Ouverte (OATAO)

OATAO is an open access repository that collects the work of some Toulouse researchers and makes it freely available over the web where possible.

This is an author's version published in: <http://oatao.univ-toulouse.fr/20501>

**Official URL:** <https://doi.org/10.1016/j.jaap.2016.10.002>

### **To cite this version:**

Morin, Mathieu and Pécate, Sébastien and Hemati, Mehrdji and Kara, Yilmaz Pyrolysis of biomass in a batch fluidized bed reactor: Effect of the pyrolysis conditions and the nature of the biomass on the physicochemical properties and the reactivity of char. (2016) Journal of Analytical and Applied Pyrolysis, 122. 511-523. ISSN 0165-2370

Any correspondance concerning this service should be sent to the repository administrator:  
[tech-oatao@listes-diff.inp-toulouse.fr](mailto:tech-oatao@listes-diff.inp-toulouse.fr)

# Pyrolysis of biomass in a batch fluidized bed reactor: Effect of the pyrolysis conditions and the nature of the biomass on the physicochemical properties and the reactivity of char

Mathieu Morin<sup>a,\*</sup>, Sébastien Pécate<sup>a</sup>, Mehrdji Hémati<sup>a</sup>, Yilmaz Kara<sup>b</sup>

<sup>a</sup> Laboratoire de Génie Chimique, Université de Toulouse, CNRS, INPT, UPS, Toulouse, France

<sup>b</sup> ENGIE Lab – Centre de Recherche et d'Innovation Gaz et Energies Nouvelles (CRIGEN) Saint Denis la Plaine, France

## A B S T R A C T

This work was carried out in order to understand the effect of the pyrolysis operating conditions and the nature of the biomass on the physicochemical properties of the char and its reactivity toward the combustion. The chars were obtained by fast pyrolysis of two types of cylindrical wood particle (beech stick: diameter of 6 mm, length of 10 mm and beech bark pellet: diameter of 10 mm, length of 15 mm) under an inert atmosphere of nitrogen in a fluidized bed reactor for three different temperatures (450, 650 and 850 °C) and at atmospheric pressure. The ultimate and FTIR analyses revealed that an increase in the pyrolysis temperature led to a raise of the carbon content and a decrease in the oxygen and hydrogen content. At high pyrolysis temperatures, Raman spectroscopy and XRD analyses showed that the char is more and more aromatic with a large size of the aromatic rings. The different chars prepared at a pyrolysis temperature of 850 °C exhibited a true density close to the one of graphite. The reactivity of chars was studied by isothermal combustion at 400 °C in TGA. The reactivity was found to be highly dependent on the pyrolysis temperature and the nature of the biomass. An increase in the pyrolysis temperature led to a decrease of the reactivity. Besides, char from fast pyrolysis of beech bark pellet is more reactive than char from fast pyrolysis of beech stick.

### Keywords:

Biomass  
Pyrolysis  
Fluidized bed  
Characterization  
Char  
Reactivity

## 1. Introduction

Biomass gasification is a promising alternative to fossil fuels for the synthesis of highly energetic products via Fischer-Tropsch or Methanation processes. It is a thermochemical conversion occurring from medium to high temperatures with many simultaneous reactions. In the case of monodisperse particles, biomass gasification is done in two steps:

(1) For temperatures up to 200 °C, the biomass is dried. Above 350 °C, biomass undergoes a thermal degradation called pyrolysis or devolatilisation occurring in the absence of oxygen which leads to the formation of volatile products either condensable (steam and tars) or non-condensable (H<sub>2</sub>, CO, CO<sub>2</sub>, CH<sub>4</sub> and C<sub>2</sub>H<sub>x</sub>) and a solid carbonaceous residue called char [1]. For instance, the product distribution of the fast pyrolysis

occurring at 850 °C is about 5% of condensable gases, 85% of non-condensable gases and 10% of char [2].

(2) Then, the char reacts with steam, oxygen or carbon dioxide in an oxidizing atmosphere at temperatures greater than 700 °C to produce syngas.

The char is a complex solid residue composed of carbon, hydrogen, oxygen and inorganic matters (ashes). The fundamental carbon structure of the char is the aromatic ring structure. The hydroaromatic and aliphatic structures account for most of hydrogen while hydroxyl (–OH), carboxyl (–COOH) and carbonyl (=CO) forms are the major oxygen functional groups [3]. For instance, Laurendeau [3] observed that a typical bituminous coal consists of a series of aromatic and hydroaromatic clusters containing an average of 2–5 rings per cluster and joined together by methylene and aliphatic linkages. Char is also a porous material composed of micropores, mesopores and macropores which are usually classified by considering three cylindrical diameter ranges  $d_{\text{pore}}$ :

- (1) Micropores:  $d_{\text{pore}} < 2 \text{ nm}$ ,
- (2) Mesopores:  $2 \text{ nm} < d_{\text{pore}} < 50 \text{ nm}$ ,

\* Corresponding author at: Laboratoire de Génie Chimique, 4 allée Emile Monso, 31432 Toulouse, France.

E-mail address: [mathieu.morin@ensiacet.fr](mailto:mathieu.morin@ensiacet.fr) (M. Morin).

### (3) Macropores: $d_{\text{pore}} > 50 \text{ nm}$ .

Biomass gasification is an endothermic process. Therefore, a contribution of energy is required to maintain a sufficient temperature in the reactor so that endothermic reactions can be carried out. Several technologies are used for biomass gasification [4–7]. These technologies can be divided into two categories depending on the mode of heat transmission:

- In the first case, the energy is provided by the partial combustion of biomass inside the reactor (in situ combustion). This first category includes: the fixed bed gasifiers (co-current – counter-current) and the “bubbling fluidized bed” gasifiers. They are used for the production of a synthesis gas that can be used for the production of heat and electricity or in cogeneration. Several mechanisms are present in these types of reactor including biomass drying and pyrolysis, the partial combustion of volatile matters and char and finally the gasification of char. Consequently, the energy necessary for the gasification is provided by the partial combustion of biomass inside the reactor [4,6,7].
- Another encouraging technology is dual or twin fluidized bed [8]. This process uses the ex situ combustion of char. Its principle relies on the circulation of a media (for instance: sand, olivine or catalyst particles) which acts as a heat carrier between an endothermic reactor and an exothermic reactor. In the former called gasifier, biomass gasification is carried out to produce syngas. In the exothermic reactor called combustor, a part of the char from the gasification process is burned to produce heat. The heat generated by the combustion provides the energy necessary for the gasification. Hence, the media soaks up the heat in the combustor to release it in the gasifier.

During these biomass gasification processes, char reacts with steam, carbon dioxide or oxygen. Thus, in order to better understand the phenomena occurring within the reactors, information concerning the influence of the nature of biomass and operating conditions of the pyrolysis step on the reactivity of char become essential. Char reactivity depends on three parameters: (1) the chemical structure of the solid, (2) inorganic matters content and (3) porosity of the particle [3]. Chemical structure of the solid promotes the formation of active sites which are highly dependent on the concentration of carbon edges, defects and dislocations as well as oxygen and hydrogen content. Inorganic constituents foster catalytic activity and further dislocations. Finally, the porosity corresponds to the total accessible surface area which control diffusion rate and the local concentration of gaseous reactants [3]. Together, these three parameters are affected by pyrolysis conditions.

Pyrolysis corresponds to a complex chemical transformation. It is well established today that operating conditions during pyrolysis of biomass – such as nature of the biomass, heating rate, final temperature, pressure, soaking time and gas atmosphere – influence the amount and the nature of volatile products and the physico-chemical properties of the produced char [1,3]. In the literature, several techniques were used to study the structure and properties of chars either from pyrolysis of coal or fewer from pyrolysis of biomass.

The heating rate has an influence on the pyrolysis products. Williams et al. [9] reported that a higher heating rate leads to the formation of lower yields of char and higher yields of gas and liquid. For instance, during the pyrolysis of pine wood at a final temperature of 720 °C, the amount of CO increases from 0.070 mol to 0.230 mol from 5 to 80 K/min, respectively [9]. The heating rate is also known to influence the char reactivity. Some authors [10–14] concluded that an increase in the heating rate increases the reactivity of char. Guerrero et al. [10] observed that a char obtained by slow pyrolysis of eucalyptus under a constant heating rate of 10 °C/min

is less reactive toward oxygen than char from fast pyrolysis in a fluidized bed reactor. The authors suggested that a higher heating rate enables higher surface area, higher oxygen and hydrogen content and higher availability of active sites. Cetin et al. [11] mentioned that the higher reactivity of char at high heating rate is due to the higher total surface areas of the char. Mermoud et al. [14] also pointed out that the char prepared at low heating rate (2.6 °C/min) is denser and has a reactivity 2.6 times lower than the char obtained at high heating rate (900 °C/min). Lu et al. [15] showed that chars prepared at low heating rate exhibit higher ordering in structure which is further developed.

The final pyrolysis temperature plays a significant role on the pyrolysis products as well as on the structure and the reactivity of char. An increase in the pyrolysis temperature increases the yield of gas and decreases the yield of char [16,17]. Liquid yields are maximized under flash pyrolysis conditions and present a maximum yield around 500 °C before decreasing. Most of the molar fractions of the component in the gas also increase [16]. Hémami et al. [18] observed that the amount of CO<sub>2</sub> is reduced by increasing pyrolysis temperature which is due to the Boudouard reaction favored at higher temperatures. The different authors [19–22] agreed that an increase in the final pyrolysis temperature leads to a decrease in the char reactivity. This is due to the improvement in structural ordering of the char and the presence of larger aromatic rings system by increasing pyrolysis temperature. By using characterization techniques such as FTIR and NMR spectroscopy, Sharma et al. [23,24] concluded that char has a higher hydrogen and oxygen content at low pyrolysis temperature (below 400 °C) and becomes more and more aromatic by increasing pyrolysis conditions.

The pyrolysis pressure has an effect on the yield of char and volatile products. For instance, an increase in the pyrolysis pressure from 1 to 5 atm increases the yields of char and CO<sub>2</sub> but decreases the yields of CO, CH<sub>4</sub> and H<sub>2</sub> [25]. According to several authors [11,26], a higher pyrolysis pressure yields to a decrease in the char reactivity. Okumura et al. [26] studied the effect of pyrolysis pressure from 0.1 to 3 MPa at 800 °C during the pyrolysis of Douglas-fir chips on the reactivity of char with carbon dioxide. They attributed the decrease of char reactivity with pyrolysis pressure to the raise of carbonaceous structure of the char. In the case of coal devolatilisation, Roberts et al. [27] concluded that char made from high pyrolysis pressure of Australian coal is more reactive towards H<sub>2</sub>O and CO<sub>2</sub> than char produced at atmospheric pressure and attributed this effect to the increase of surface area at high pyrolysis pressure.

The soaking time corresponds to the residence time of the char at the final pyrolysis temperature. Some authors studied the effect of this parameter on the char reactivity [12,14,28,29]. After biomass devolatilisation, the residence time at the final pyrolysis temperature leads to the modification of the solid structure of the char which influences the reactivity. According to several researchers [12,28], this time decreases the char reactivity. For instance, Kumar et al. [12] observed that the reactivity of both acacia and eucalyptus chars decreases as the soaking time increases. This phenomenon is also called thermal annealing. This is due to the fact that prolonged heating at the final pyrolysis temperature improves structural ordering of the char and the loss of active sites. By carrying out slow and fast pyrolysis of wood and agricultural residues, Zanzi et al. [28] concluded that char obtained by rapid pyrolysis contains a fraction that can be volatilized further by slow pyrolysis. Consequently, the authors divided the pyrolysis into two steps: an initial fast pyrolysis step completed within seconds followed by a slower step including some chemical rearrangements of the char which takes several minutes to be completed. Senneca et al. [29] studied the effect of carbonization time – from 1 to 300 min – at a given temperature of a bituminous coal on the reactivity with carbon dioxide. They found that thermal annealing has a larger effect in the early stage of the char gasification and vanished at conversion

greater than 0.55. They suggested that both gasification and thermal annealing occurs together during gasification of char. However, Mermoud et al. [14] studied the reactivity of char obtained by fast pyrolysis of beech at 927 °C with a soaking time of 8 min and 1 h. They noted no difference in the gasification kinetic and concluded that beech char does not undergo thermal annealing at pyrolysis temperature of 927 °C in duration up to 1 h.

Regarding the influence of biomass nature on the pyrolysis products, different authors [18] concluded that this parameter does not have a significant effect on the composition of the non-condensable gases. For instance, Hémati et al. [18] carried out fast pyrolysis of beech and pine sawdust at 850 °C in fluidized bed reactor. In the case of beech sawdust, they showed that the molar fractions of H<sub>2</sub>, CO, CO<sub>2</sub>, CH<sub>4</sub> and C<sub>2</sub>H<sub>6</sub> were 19%, 53.2%, 8%, 13% and 5% respectively and these fractions did not significantly vary for pyrolysis of pine sawdust. However, the nature of the initial biomass is a determining parameter concerning the structure and properties of the produced char as well as its reactivity. The reactivity of char from different raw materials can significantly vary. Several parameters are believed to be responsible for this variation and are still investigated in the literature.

The amount of ash seems to be determining as it is known to catalyze the reaction of gasification [12,14,20]. However, its effect is not well-established yet. Some authors observed a difference in char reactivity in combustion for various coals with different ash content but the catalytic effect of mineral matter could not be demonstrated [30]. Nevertheless, according to Asadullah et al. [19], the structure of char plays a more dominant role than the catalytic effect of the ash in char combustion reactivity.

Another parameter which strongly influences the reactivity is the char structure (density, surface area, pore size distribution and porosity). It can be measured by a variety of methods. The three main methods are pycnometry, mercury porosimetry and adsorption [3].

Helium pycnometry technique is used to measure the true density of char while mercury porosimetry is performed to determine the apparent density and the pore size distribution of the solid.

The determination of the surface area by adsorption technique remains difficult. The main gases used for physical adsorption are N<sub>2</sub> at 77 K and CO<sub>2</sub> at 273 K. For adsorption of N<sub>2</sub> at 77 K, it is well known that nitrogen diffusion in the micropores is very slow and equilibrium cannot sometimes be achieved [3,11]. Laurendeau [3] reported that nitrogen cannot penetrate through pores with  $d_{\text{pore}} < 500$  nm. In the case of CO<sub>2</sub> adsorption at 273 K, carbon dioxide can penetrate through capillaries because of polar interactions with char surface. Some authors [11] compared the results of CO<sub>2</sub> and N<sub>2</sub> surface area of chars and reported that sample with high CO<sub>2</sub> but low N<sub>2</sub> surface areas may indicate the high magnitude of micropores while those with similar N<sub>2</sub> and CO<sub>2</sub> surface areas may suggest the existence of larger pore structures.

Char surface area was widely investigated in the literature [11,13,31–33]. The authors concluded that macropores and mesopores surface area is the only parameter which participates to the reaction while micropores surface area is not a good indicator. Fushimi et al. [13] considered that macropores in the char are more accessible to the reactant and provides more active sites than micropores. According to Cetin et al. [11] the macropores are the result of melting of the char particles, especially at high heating rate. This observation is in good agreement with the work of Hurt et al. [31]. Consequently, some authors [14] concluded that the surface area determined by mercury porosimetry gives better results to correlate reactivity of chars.

In the gasification process, char reacts with steam, carbon dioxide or oxygen. To study the reactivity of chars, the different researchers used one of these three gasifying agents and different types of reactor (for instance: tubular reactor [11,24], TGA

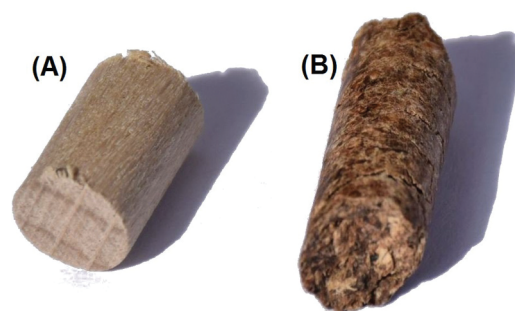


Fig. 1. Picture of the two biomasses, (A) beech stick and (B) beech bark pellet.

[12–14,19,26,28] and quartz reactor [34]). In this work, we study the reactivity by isothermal combustion of char in TGA. In addition to chemical structure, inorganic matters content and porosity, the reactivity also depends on the size of the particles, the gasification temperature and the reactant partial pressure. During the combustion, several steps occur: the external transfer of oxygen from the bulk to the external surface of the particle, diffusion of oxygen within the pores of the solid and finally the intrinsic chemical reaction. Thus, the reaction may be divided into three main regimes according to the combustion temperature [35]. In Regime I (low temperatures region), the intrinsic reactivity of the solid is low with respect to oxygen diffusion inside the pore and external transfer around the particle. The Regime II (medium temperatures region) is the transition regime where both the diffusion of oxygen and the intrinsic chemical reaction play an important role. In Regime III (high temperatures region), the intrinsic reactivity of the solid is very high and oxygen molecules react at the particle surface as soon as they pass the boundary layer around the particle. External mass transfer is then the limiting step. In this work, we carried out isothermal combustion in Regime I.

The aim of the present study is to thoroughly understand the physicochemical changes in the char structure and properties during the pyrolysis of two types of biomass. This article will be divided into two parts.

- (1) In the first part, the characterization of chars obtained from fast pyrolysis of biomass at three different temperatures is investigated. The pyrolysis is carried out in a batch fluidized bed reactor at different temperatures ranging from 450 to 850 °C and at atmospheric pressure. The produced chars were characterized by Scanning Electron Microscopy (SEM), Fourier Transform Infrared (FTIR), Raman spectroscopy and X-Ray diffraction (XRD).
- (2) In the second part, the reactivity of the different chars is studied by isothermal combustion in TGA at 400 °C. The purpose is to observe the influence of the pyrolysis temperature and the nature of the biomass on the char reactivity.

## 2. Experimental section

### 2.1. Char preparation

The biomasses used in this work are cylindrical pellets of beech bark ( $D = 6$  mm,  $L = 15$  mm) obtained by mechanical compaction of sawdust, and beech stick ( $D = 6$  mm,  $L = 10$  mm). A picture of the raw materials is given in Fig. 1. The proximate analysis of the two biomasses was carried out following the standard test method for chemical analysis of wood charcoal D 1762–84. The results are presented in Table 1.

Fast pyrolysis of the two types of biomass was carried out under an inert atmosphere of nitrogen by instant immersion of a fixed

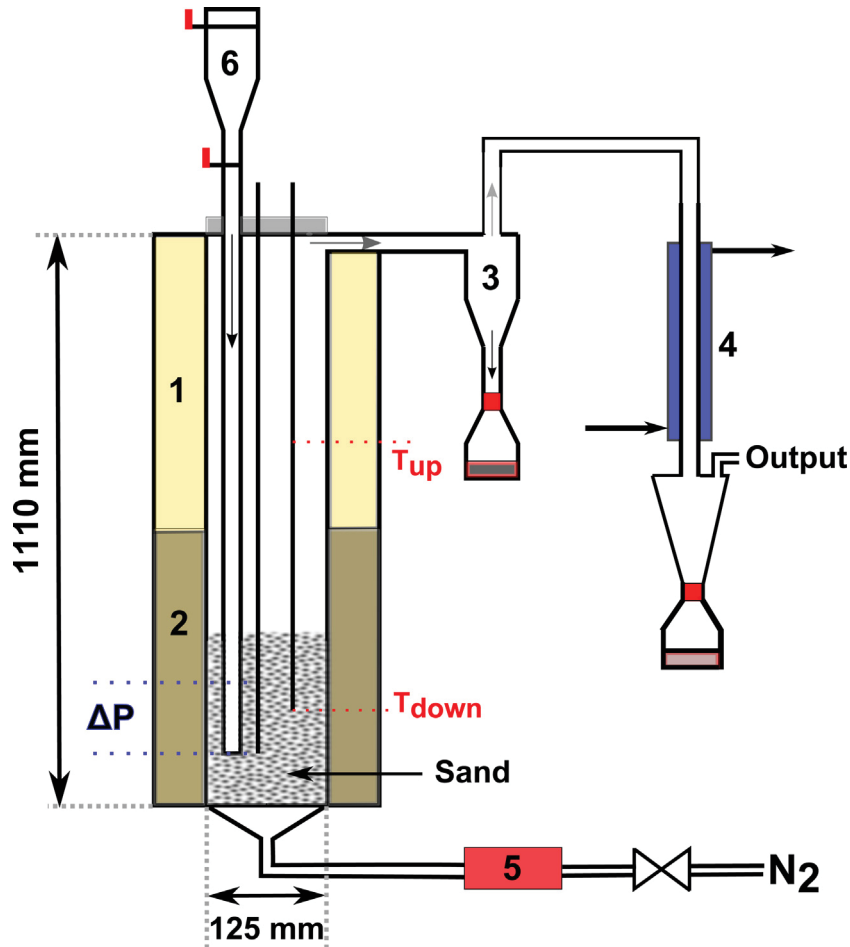


Fig. 2. Experimental rig for biomass pyrolysis, 1: Furnace 1, 2: Furnace 2, 3: Cyclone, 4: Condenser, 5: Rotameter, 6: Biomass sealed container.

Table 1  
Proximate analysis of the biomasses.

Biomass	Moisture (%)	Volatile matters (%)	Fixed carbon <sup>a</sup> (%)	Ash (%)
Beech bark pellet	9.80	75.13	12.25	2.82
Beech stick	7.74	76.7	15.36	0.2

<sup>a</sup> By difference.

mass of biomass particles in a batch dense fluidized bed (Fig. 2) containing 5 kg of inert hot particles (sand,  $d_{32} = 249 \mu\text{m}$ ). This reactor is made of a refractory steel cylindrical tube with 125 mm inner diameter and 1110 mm height. It is surrounded by two electric furnaces having 6 kW electric powers. Reactor temperature is controlled using a P&ID controller. The gas distributor is a refractory steel perforated plate with a porosity of 0.5%. The fluidizing gas flow rate is measured by a rotameter before feeding the bed. At the column outlet the elutriated particles and condensable vapors are collected respectively by a cyclone and a condenser. The biomass injection system consists of a cylindrical tube of 25 mm in diameter with the lower end located within the fluidized bed. It is connected by a valve to a sealed container containing a well-defined mass of biomass. The reactor is equipped with two K thermocouples located at 225 and 650 mm above the distributor and a differential pressure transmitter ( $\pm 0.1$  mbar).

The experiments are carried out with fixed nitrogen mass flow rate of 7 kg/h, corresponding respectively to 4.5 and 7 times the minimum fluidization velocity of sand at 450 and 850 °C.

The injected biomass mass is chosen to ensure that pyrolysis operation stays isothermal. A preliminary study, performed with

different biomass masses has shown that the sample mass should not exceed 20 g to prevent a temperature decrease superior to 5 °C.

The fast pyrolysis of the two biomasses was carried out at 450, 650 and 850 °C at atmospheric pressure. After reaching the pyrolysis temperature, about 20 g of biomass are introduced inside the fluidized bed and the operation is repeated at least 5 times to produce a significant amount of chars. To make the comparison possible between the different chars, the soaking time at bed temperature was kept identical for each of the studied temperatures. It is approximately 3 h. A study on the temporal variation of the biomass particle center temperature during its introduction in the fluidized bed reactor was performed (not presented in this paper) and showed that the heating rate of the beech stick and beech bark pellet center is respectively 374 and 305 °C/min at 450 °C and 1062 and 873 °C/min at 650 °C. The heating rate of the particle was determined experimentally by the difference between the temperature of the beginning of hemicellulose degradation which takes place for temperatures around 225 °C and the temperature corresponding to the end of the lignin degradation (around 400 °C) divided by the time. Due to a strong particle size reduction, the heating rate during the pyrolysis at 850 °C could not be determined. After the pyrolysis, the produced chars were cooled under a flow of nitrogen before being recovered the day after by sieving. They were stored inside a pill-box until they were analyzed. Pellet chars have a structure made of an agglomeration of fine elementary particles with the presence of numerous pores while stick chars also consist of a compact structure made of open pores which continue inside the particle. Information regarding the diameter – length of the obtained char particles were directly measured and aver-

**Table 2**  
Ultimate analysis and properties of the different chars.

Materials	Pyrolysis conditions			Char form D(mm)–L(mm)	True density (kg/m <sup>3</sup> ) He	Ultimate analysis (db, wt%)				Chemical Formula
	Biomass type	Pyrolysis Temp. (°C)	Heating rate (°C/min)			C	H	O	Ash	
PEL	Beech bark	–	–	6–15	1433.3	44.79	6.09	47.29	2.82	CH <sub>1.63</sub> O <sub>0.79</sub>
PEL450	Beech bark	450	305	4–10	1504.2	74.47	2.99	12.88	8.59	CH <sub>0.48</sub> O <sub>0.13</sub>
PEL650	Beech bark	650	873	4–9	1722.8	75.62	2.03	8.98	10.85	CH <sub>0.32</sub> O <sub>0.09</sub>
PEL850	Beech bark	850	–	2–6	1832.5	75.49	0.56	6.06	12.05	CH <sub>0.09</sub> O <sub>0.06</sub>
STI	Beech	–	–	5–10	1362.5	44.63	6.37	45.24	0.20	CH <sub>1.71</sub> O <sub>0.76</sub>
STI450	Beech	450	374	4–10	1394.3	74.10	4.17	18.96	1.17	CH <sub>0.68</sub> O <sub>0.19</sub>
STI650	Beech	650	1062	4–9	1589.4	84.47	2.75	7.39	3.20	CH <sub>0.39</sub> O <sub>0.07</sub>
STI850	Beech	850	–	2–8	1924.4	87.64	0.57	6.95	2.79	CH <sub>0.08</sub> O <sub>0.06</sub>

age values are given in Table 2. The shape of chars obtained at 450 and 650 °C remains cylindrical with a small decrease of the diameter and length compared to the initial biomass which is due to the pyrolysis intensity and particles attrition in the fluidized bed. Particularly, chars from pyrolysis at 450 °C are very close to the initial biomass. As the pyrolysis temperature increases, the size of the chars decreases and the structure seems more breakable. At 850 °C, the shape of the chars consists of a cylinder chopped in the longitudinal direction.

After the pyrolysis at 650 °C, the weight of the produced char (recovered by sieving) was measured and the char production rate was determined. It was about 11%. However, this value is underestimated due to intense mixing between the fluidized media and char particles. This phenomenon can lead to attrition and fragmentation of char and the production of fine particles which were not taken into account in the calculation of the char production rate.

## 2.2. Characterization methods

Prior to characterization tests, the different chars were grinded and homogenized to ensure that all samples have the same properties. The mean surface diameter ( $d_{32}$ ) of the grinded char particles is 25  $\mu\text{m}$ .

The chars were analyzed in order to determine their physico-chemical properties:

- the true density of chars by helium pycnometer,
- the ultimate analysis was performed at “the Institute of Analytical Science” in Lyon (France) to determine the C, H and O contents.
- The structure morphology of char was obtained through Scanning Electron Microscopy analysis using a SEM FEG JSM 7100FTLS by JEOL at the “Laboratoire de Génie Chimique”. The analyses were performed on the samples previously coated with gold 10 nanometer Au/Pd film.
- The Infrared spectra were recorded in absorbance mode on Tensor 27 instrument connected to a Digitec™ DLaTGS detector high sensibility. Typically 2 mg of grinded char sample were blended into 200 mg of KBr to form standard pellets for FTIR analysis. A spectrum resolution of 4  $\text{cm}^{-1}$  was used and the spectra were recorded from 400 to 4000  $\text{cm}^{-1}$ .
- The XRD analysis was carried out with a Bruker instrument to examine the carbon structure of the different chars. The wavelength of the X-ray diffraction is 1.5418 Å.
- The Raman analyses were performed in air at room temperature using an Horiba Jobin Yvon Labram HR 800 spectrometer equipped with an He/Ne laser at 633 nm at the “Centre Inter-universitaire de Recherche et d'Ingénierie des Matériaux” (France). A laser power of 7 MW was selected. The spectrum of

each sample was acquired through a grating of 600 tr/mm with a spectral resolution of 2  $\text{cm}^{-1}$ . As char can be heated up easily in the laser beam, a filter was used to avoid any degradation of the sample. The final method selected to perform Raman analysis uses two filters, microscope lens  $\times 100$ , 60 s of exposition time and 2 accumulations.

Char reactivity in combustion was determined using isothermal TGA analyses with a TGA Q600 analyzer from TA instruments. Preliminary tests with various sample weights ranging from 2 to 15 mg confirmed that 8–10 mg is the optimum sample weight which enables to achieve accurate and repeatable results. Consequently, about 10 mg of chars were introduced inside an alumina crucible (inner diameter and height of the crucible equal to 5.5 mm and 4 mm, respectively) for each test. The experimental protocol is divided into two stages. The first one, carried out under high-purity nitrogen flow (100 NmL/min), consists of:

- an initial period of 15 min at ambient temperature used to purge the air from the system,
- a linear heating rate of 10 °C/min from ambient temperature to the run temperature (400 °C),
- a period of 15 min at the run temperature to stabilize the system.

The second stage is the isothermal combustion carried out by switching nitrogen to air with the same flow rate. The experiments are performed at 400 °C. The choice of this temperature is discussed in Section 3.6.1.

The temporal conversion rate is calculated via the evolution of sample weight versus time as follow:

$$X = \frac{w_i - w(t)}{w_i - w_{ash}} \quad (1)$$

Where  $w_i$ ,  $w_{ash}$  and  $w(t)$  are the values of the initial, final, and temporal mass of the sample, respectively.

The apparent reaction rate was defined as the derivative of the evolution of the conversion rate versus time, for a conversion rate of 50%:

$$R_{app} = \left. \frac{dX}{dt} \right|_{x=0.5} \quad (2)$$

## 3. Results and discussions

### 3.1. Ultimate analysis and char properties

Table 2 reports the C, H, O and ash contents and the true density of the raw material and the different chars obtained from fast pyrolysis and for various temperatures. It can be seen that the two biomasses have a carbon, hydrogen and oxygen content in the same

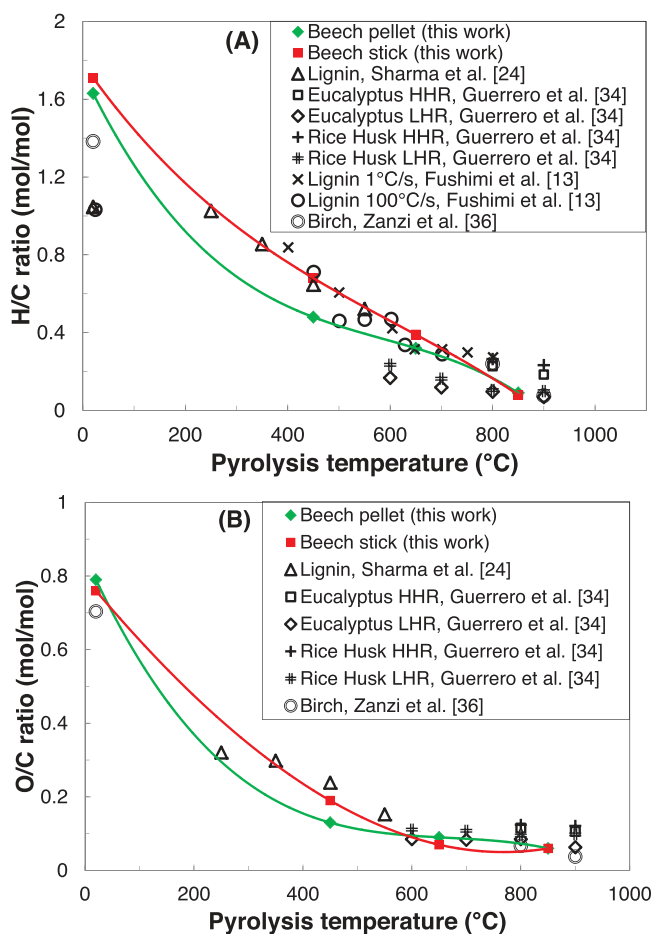


**Fig. 3.** Variation in elemental composition of different chars versus pyrolysis temperature and comparison with results from the literature works, (A) H/C molar ratio, (B) O/C molar ratio [36].

order of magnitude. This table also shows that a higher pyrolysis temperature results in higher carbon content and lower hydrogen and oxygen content. As can be observed, the carbon content is higher for stick chars than pellet chars. Likewise, the hydrogen and oxygen content is lower for pellet chars than stick chars. The oxygen and hydrogen contents in the char can be related to the availability of active sites and are believed to influence the overall reactivity in combustion [3].

As carbon, hydrogen and oxygen are always detected, the char cannot be considered as pure carbon and should be expressed in the form of  $\text{CH}_x\text{O}_y$ .

A higher amount of ash is also observed for the pellet chars which is mainly composed of calcium, potassium and silica. This high quantity of ash is due to the presence of beech bark. The true density of chars slightly increases for temperatures up to 450 °C. This indicates a partial degradation of the wood. By increasing pyrolysis temperature above 450 °C, the true density substantially increases to approach the true density of amorphous carbon and graphite ( $\rho_{\text{t,graphite}} = 2000\text{--}2200 \text{ kg/m}^3$ ).

Fig. 3 presents the variation in elemental composition during the pyrolysis. In the same figure are also presented the results of different works from the literature. The H/C and O/C molar ratios substantially decrease by increasing pyrolysis temperature. This shows that the char contains a higher amount of carbon and a lower amount of hydrogen and oxygen as the pyrolysis temperature increases. Above 400 °C, a similar trend is observed for the H/C and O/C molar ratios of different works in the literature. This suggests that the nature of the initial raw material and the pyroly-

sis heating rate have only a small influence on the composition of chars for temperatures higher than 400 °C. Fushimi et al. [13] reported that the decrease in the H/C ratio up to 650 °C is due to the devolatilisation of aliphatic groups while at higher temperatures, the decrease is attributed to the aromatization and carbonization of the char.

### 3.2. SEM analysis

Fig. 4 illustrates SEM analysis of the beech bark pellet and its associated chars obtained under different pyrolysis temperatures. The beech bark pellet exhibits a structure of numerous typical wood fibers aligned in the longitudinal direction having an approximately diameter of 10  $\mu\text{m}$ . Biomass chars consist of different morphologies according to pyrolysis conditions. For pyrolysis temperatures in the range of 450–650 °C, the presence of smooth regions which correspond to the carbonized wood fibers reveals that the particles have melted. Melting phenomenon was noticed by researchers in the literature [11,23]. Cetin et al. [11] concluded that at atmospheric pressure, the particle first swells, followed by the melting and the evolution into a droplet before rupturing and losing its volatile products. This conclusion is in good accordance with the work of Sharma et al. [23] who divided pyrolysis of pectin into three stages: the initial melting of the particle followed by the release of the volatile matters and the formation of vesicles.

The structure of chars also exhibits some disorder such as surface etchings (Fig. 4(B) and (C)). A raise in the pyrolysis temperature causes significant transformation to the surface morphology of the char. The emission of volatile products leads to the formation of vesicles (bubbles), open and close pores (Fig. 4(D)). At high pyrolysis temperature, structure seems more breakable and open pores seem to vanish. Some researchers [34] concluded that a loss of the original morphology can lead micropores to collapse and decrease the surface area of char.

Fig. 5 shows SEM pictures of beech stick and its chars produced from different pyrolysis temperatures. It can be seen that beech stick is compact and consists of irregular particles with slit-shaped surfaces that provide an internal porous structure. At low pyrolysis temperature, no significant morphological variations are present compared to the raw material. The char is made of open pores which seem to continue inside the particles and illustrate the result of the volatile components being released in the longitudinal direction (Fig. 5(B)). As the temperature is increased from 450 to 850 °C, open bubbles in the surface of the bounded cells show a breakable char with more open structure and thinner cell walls. Besides, chars obtained from beech bark pellet pyrolysis developed a more disordered structure than those obtained by beech stick pyrolysis. This is due to the difference in structure of the initial biomass since beech bark pellet is made of mechanical compaction of sawdust beech bark.

### 3.3. FTIR analysis

Fig. 6 compares the FTIR spectrum of the initial beech bark pellet and its associated chars obtained by pyrolysis at 450, 650 and 850 °C. The spectrum has been corrected for atmospheric  $\text{CO}_2$  and water vapor contributions. For the beech bark pellet, the main bands are the strong hydrogen bonded O–H stretching absorption at wavenumbers around 3400  $\text{cm}^{-1}$ , the C–H stretching (aliphatic C–H) at 2940  $\text{cm}^{-1}$ , the symmetric C–H<sub>3</sub> stretch (methoxyl group) around 2870  $\text{cm}^{-1}$ , the C=O stretch (carbonyl group) at 1730  $\text{cm}^{-1}$  and the aromatic skeletal vibration of benzene ring at wavenumber of 1505  $\text{cm}^{-1}$ . In the region of 1800–900  $\text{cm}^{-1}$ , several bands are observed corresponding to the various functional groups of cellulose, hemicellulose and lignin. The intensity of these bands depends on the proportion of these three components. The band

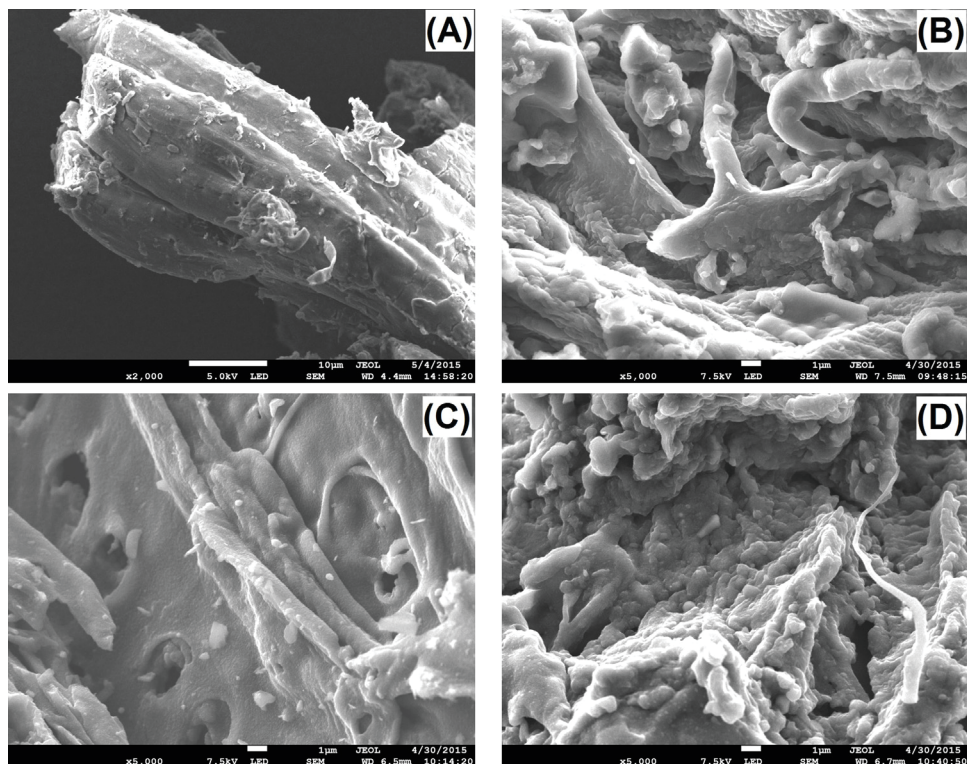


**Fig. 4.** SEM images of (A) Beech bark pellet, and char from fast pyrolysis of beech bark pellet in a fluidized bed reactor at (B) 450 °C, (C) 650 °C, (D) 850 °C.

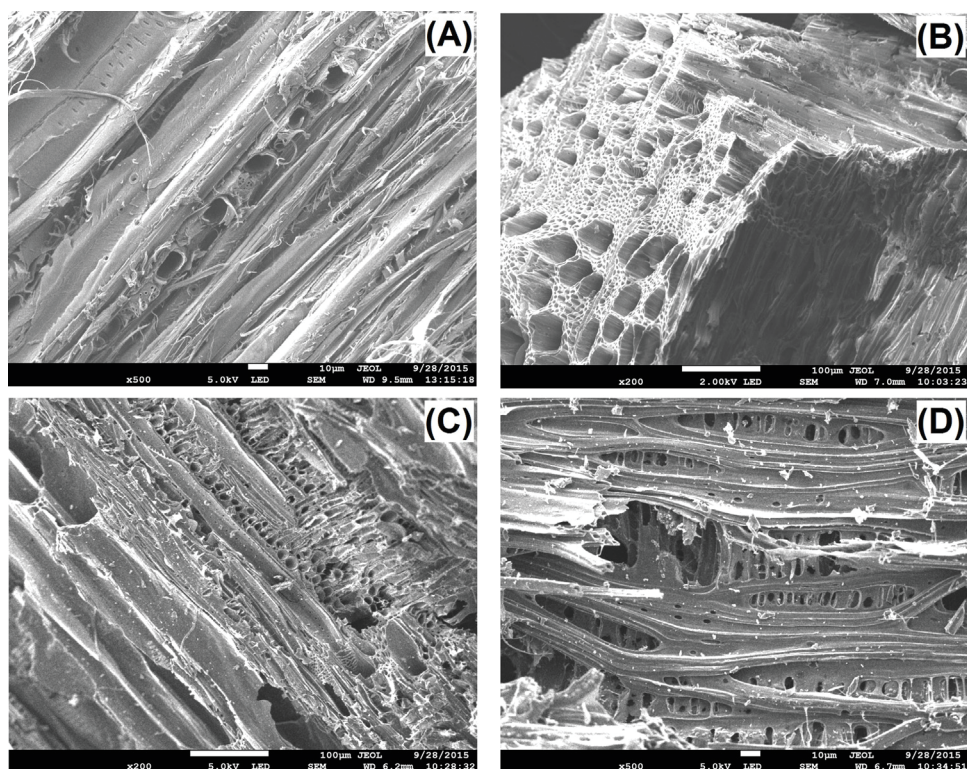


**Fig. 5.** SEM images of (A) beech stick, and char from fast pyrolysis of beech stick in a fluidized bed reactor at (B) 450 °C, (C) 650 °C, (D) 850 °C.

at wavenumbers of  $1610\text{cm}^{-1}$  is due to the aromatic skeletal vibration breathing with C=O stretching and between  $1030$  and  $1300\text{cm}^{-1}$ , the bands are associated with the presence of guaiacyl and syringyl rings [37,38]. For instance, the strong band at wavenumbers of  $1030\text{cm}^{-1}$  is associated with the C–H deforma-

tion in guaiacyl with C–O deformation in primary alcohol due to the presence of methoxyl group. Finally, the bands between  $900$  and  $700\text{cm}^{-1}$  are attributed to aromatic C–H out-of-plane [23].

An increase in the pyrolysis temperature results in a less complex spectrum with a continuous decrease in intensity for many

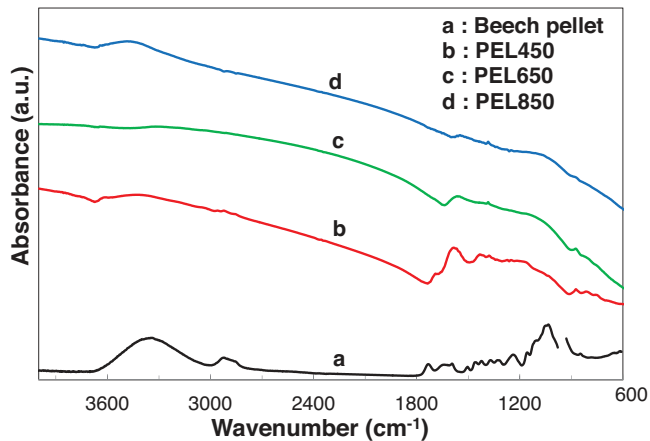


Fig. 6. FTIR spectrum of beech bark pellet and its associated chars obtained from pyrolysis at 450, 650 and 850 °C.

bands. The absence of most bands suggests that the char is mainly carbonized. An obvious decrease is observed for stretches due to C=O (carbonyl groups), C–H (aliphatic groups), C–H<sub>3</sub> (methoxyl group) and aromatic C–H. The latter is attributed to the loss of peripheral hydrogen and suggests that the char is mainly composed of carbon above 650 °C. Most of the bands in the region of 1030 and 1300 cm<sup>-1</sup> totally vanished. Intensity of the hydroxyl groups (O–H) is variable with pyrolysis temperature and is associated with the presence of H<sub>2</sub>O adsorbed in the char structure. Besides, results in Fig. 6 show an increasingly upward drift in baseline at high wavenumbers. Some authors [23,24] attributed this increase to the raise in the aromatic carbon content of the chars. Other researchers also observed these changes in FTIR spectra for different pyrolysis temperatures and concluded that the char become more and more aromatic as the pyrolysis temperature increases [23,24,39]. Same conclusions can be drawn for the FTIR spectra of beech stick and beech chars.

### 3.4. X-Ray diffraction

The structural properties of the different chars were examined by X-ray diffraction. XRD analysis is a useful tool to provide information regarding the crystallinity and the presence of aromatic layers since they directly influence the reactivity of char towards the combustion and gasification.

Fig. 7 presents the diffraction curves of pellet chars prepared from different pyrolysis temperatures. Pellet chars have strong and narrow bands over the examined 2θ which are associated with the presence of inorganic matters in the carbon matrix. This last result is in good agreement with ultimate analysis (Table 2) which shows a higher amount of ash in pellet chars. The features of interest in this work are the two broad bands observed at 2θ approximately equal to 24° and 44°. The (002) peak is located at 24° and is attributed to the stacking of the graphitic basal plans of char crystallites [11,15]. Some authors [34,15] mentioned the apparent asymmetry of the (002) peak due to the existence of the γ band on the left-hand side which is related to the packing of the saturated structures such as aliphatic side chains. The (100) band centered at 44° is associated with the hexagonal ring structure in char crystallite [15]. The aromatic layer stacking height  $L_c$  and the radial spread  $L_a$  can be expressed from the XRD spectra by using the Scherrer equation:

$$L_c = \frac{0.89\lambda}{B_{002} \cos \theta_{002}} \quad (3)$$

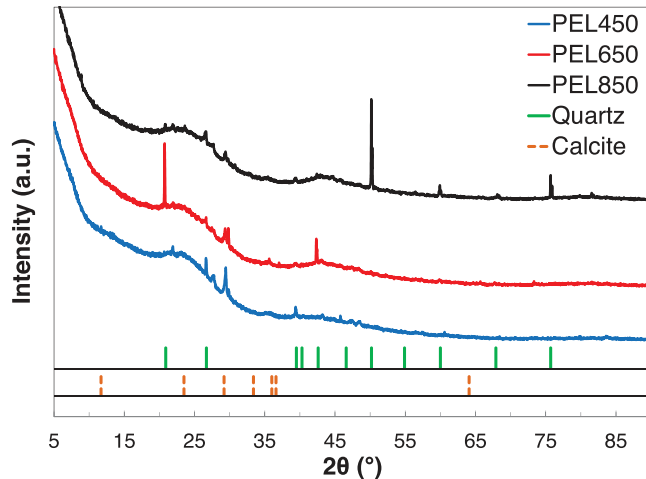


Fig. 7. Effect of the pyrolysis temperature on the XRD spectrum of chars from pyrolysis of beech bark pellet.

$$L_a = \frac{1.84\lambda}{B_{100} \cos \theta_{100}} \quad (4)$$

Where  $\lambda$  is the wavelength of the X-ray radiation (Å),  $B_{002}$  and  $B_{100}$  are the width of the (002) and (100) peak at half-maximum intensity respectively (Rad) and  $\theta_{002}$  and  $\theta_{100}$  are the peak position (°).

The presence of the (002) and (100) bands in the spectra suggests that the crystallites in the char have an intermediate structure between amorphous carbon and aromatic carbon. Some authors assigned the background intensity to amorphous carbon [11,15,34]. It can be seen that, at low pyrolysis temperatures, the (002) and (100) bands are broad. Therefore, the size of the carbon crystallites in the char is small and poorly aligned due to the cross-linked [20]. By increasing pyrolysis temperature, several observations can be made:

1. The (002) and (100) bands seem to sharpen and narrow. By referring to Eq. (3), the aromatic layer stacking height  $L_c$  becomes larger. This indicates a more ordered carbon structure and an increase of the crystallite size.
2. The background intensity of the spectra decreases indicating a reduction of the amorphous carbon content in the char. This trend was observed for each spectrum but was not shown in Fig. 7 to enable better interpretation of the spectra. Amorphous carbon represents the non-aromatic carbon trapped in the char macromolecules [15]. When the char is heated to a higher pyrolysis temperature, a higher amount of amorphous carbon is released as volatile products.
3. The (002) peak becomes more symmetric and the γ peak progressively disappears. At high pyrolysis temperature, the weak bounds between the aliphatic side chains and the carbon crystallites are broken. Aliphatic side chains are then released as volatile products.

Finally, at high pyrolysis temperatures, the char contains some ordering structure which can be attributed to aromatic rings. The size of these aromatic rings approaches a graphitic structure but cannot be considered as graphite given the significant width of the bands.

Fig. 8 presents the effects of biomass nature on the char structure during the fast pyrolysis at 850 °C. In this Figure, the baseline of the XRD spectrum has been corrected in order to enable better comparison. A little difference is observed between the two chars. ST1850 exhibits sharper, more intense and more symmetric (002)

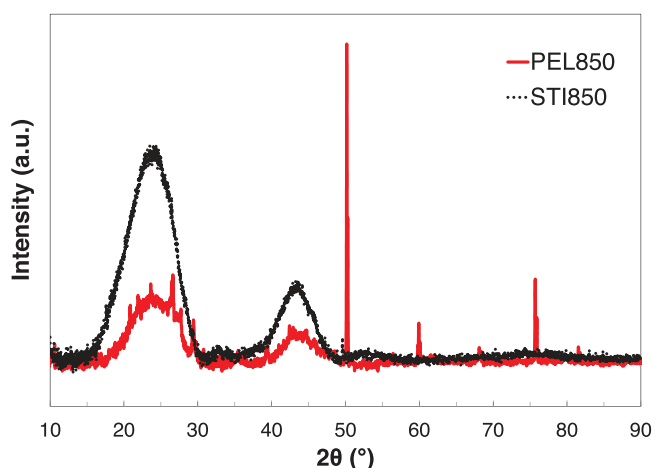


**Fig. 8.** Effect of the nature of the biomass on the XRD profile, pyrolysis of beech stick and beech bark pellet at 850 °C.

band than PEL850. It can be concluded that pellet chars have a more amorphous structure with a higher amount of aliphatic side chains than stick chars.

### 3.5. Raman spectroscopy

Raman spectroscopy is widely used in the literature to investigate the structure feature of carbonaceous materials and coal derived products [19,40,41]. The Raman spectra of single crystals of graphite show one single, strong band at 1575  $\text{cm}^{-1}$  designated as the G band due to the  $E_{2g}$  vibrational modes [42]. For disordered and amorphous carbon such as activated carbon or chars, an additional band appears at 1380  $\text{cm}^{-1}$  denoted as the D band. The origin of the D band is not well understood and might be due to the increase of the amount of unorganized carbon in the sample [34]. It is expected that the D band will disappear for compounds having an infinite sized aromatic cluster such as the graphitic structure.

Two procedures are carried out in the literature to interpret Raman spectra. In the works of Li et al. [43], the coal char did not show any signs of graphitic structures (XRD curves not shown in the papers). The authors have curved-fitted the spectra into 10 Gaussian bands by assuming that the G band is associated with the aromatic quadrant ring breathing and the D band is assigned to the aromatic rings with a ring size of no less than 6 fused benzene rings. These 10 bands are briefly summarized in Table 3. The second point of view is to consider a graphitic structure in the char. Therefore, the Raman spectra are curved-fitted into 4 Lorentzian and 1 Gaussian peaks following the method of Sadezki et al. [44].

As the XRD spectra presented above did not reveal any convincing sign of graphitic structure but rather a mixture of amorphous and aromatic carbon, Raman spectra were analyzed following the method proposed by Li et al. [43]. Fig. 9(A) shows an example of Raman spectra of char from pyrolysis of beech bark pellet at 450 °C and the curve-fitting into 10 Gaussian peaks to obtain quantitative parameters. Two broad Raman bands can be discerned at approximately 1350 and 1600  $\text{cm}^{-1}$  attributed to the D and G band respectively.

Fig. 9(B) and (C) illustrate the  $I_D/I_G$  ratio and the ratio between the D band and the ( $G_R + V_L + V_R$ ) bands in term of pyrolysis temperature. The increase in the  $I_D/I_G$  ratio with pyrolysis temperature indicates the increase in the concentrations of aromatic rings having at least six fused benzene rings. This is due to the dehydrogenation of hydroaromatics and the raise of aromatic rings in the char. The three bands  $G_R$ ,  $V_L$  and  $V_R$  stand for the typical structures found in amorphous carbon materials, especially the small aromatic

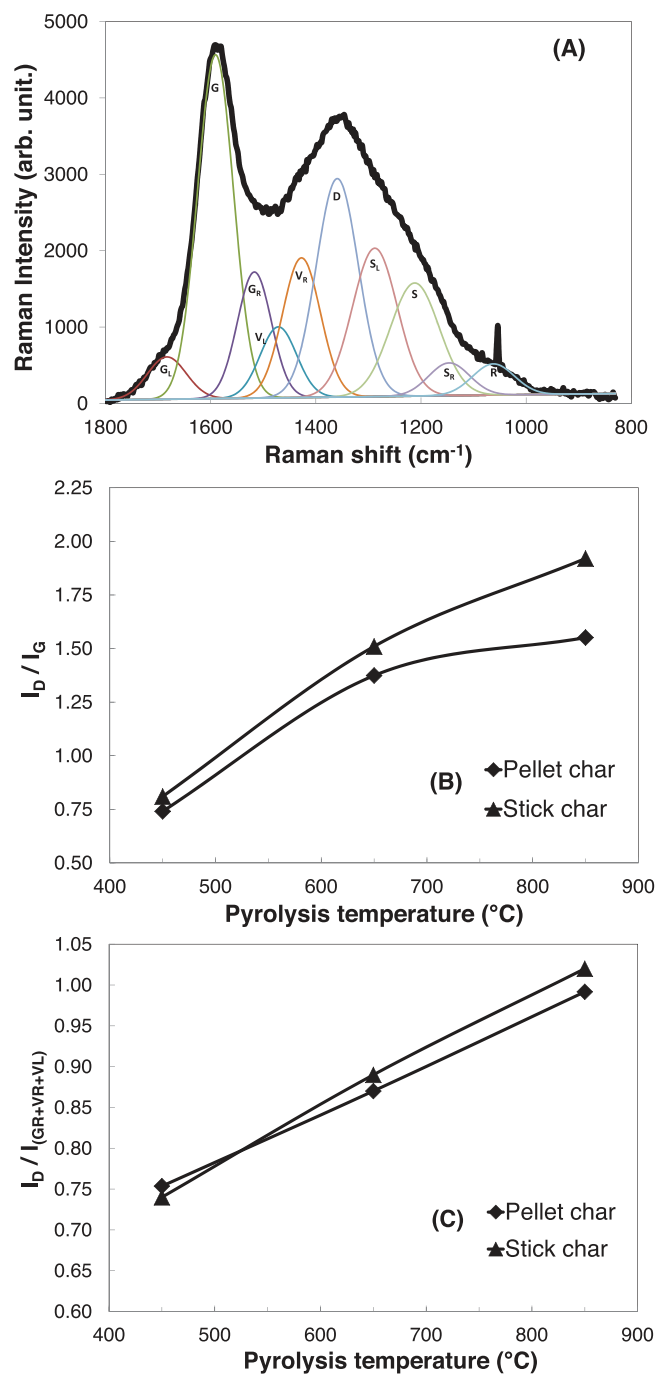


**Fig. 9.** (A) Curve-fitting of a Raman spectrum of char obtained by pyrolysis of beech bark pellet at 450 °C, (B) and (C) Band ratio as a function of pyrolysis temperature for beech bark pellet and beech stick chars.

ring systems having 3–5 fused benzene rings. Hence, the increase in the ratio observed in Fig. 9(C) is taken as a raise in the presence of large aromatic ring systems. Finally, the number of aromatic rings per ordered cluster increases by raising pyrolysis temperature.

### 3.6. Study of char reactivity: isothermal combustion of char in TGA

In this part, each experiment was conducted with char particles finely grinded. The average size of these particles is  $d_{32} = 25 \mu\text{m}$ .

**Table 3**  
Summary of peak/band assignment [43].

Band name	Band position, $\text{cm}^{-1}$	Description	Bond type
$G_L$	1700	Carbonyl group C=O	$sp^2$
G	1590	Graphite $E_{2g}^2$ ; aromatic ring quadrant breathing; alkene C=C	$sp^2$
$G_R$	1540	Aromatic with 3–5 rings; amorphous carbon structures	$sp^2$
$V_L$	1465	Methylene or methyl; semi-circle breathing of aromatic rings; amorphous carbon structures	$sp^2, sp^3$
$V_R$	1380	Methyl group; semi-circle breathing of aromatic rings; amorphous carbon structures	$sp^2, sp^3$
D	1300	D band on highly ordered carbonaceous materials; C–C between aromatic rings and aromatics with not less than 6 rings	$sp^2$
$S_L$	1230	Aryl-alkyl ether; <i>para</i> -aromatics	$sp^2, sp^3$
S	1185	$C_{\text{aromatic}}-C_{\text{alkyl}}$ ; aromatic (aliphatic) ethers; C–C on hydroaromatic rings; hexagonal diamond carbon $sp^3$ ; C–H on aromatic rings	$sp^2, sp^3$
$S_R$	1060	C–H on aromatic rings; benzene ( <i>ortho</i> -di-substituted) ring	$sp^2$
R	960–800	C–C on alkanes and cyclic alkanes; C–H on aromatic rings	$sp^2, sp^3$

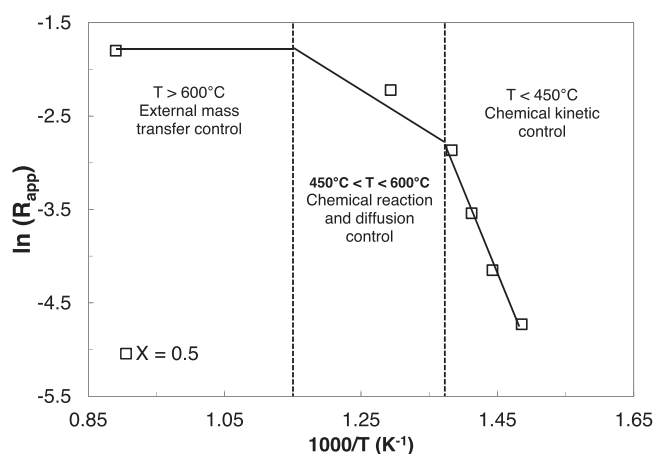


**Fig. 10.** Logarithm of apparent reactivity versus  $1/T$  for STI850 at a given conversion rate of 0.5.

### 3.6.1. Choice of isothermal combustion temperature

In order to choose the temperature of the study, the isothermal combustion of STI850 was performed at different temperatures ranging from 330 °C to 850 °C. It was found that the conversion rate is strongly dependent on combustion temperature. As the combustion temperature increases, the conversion rate increases. For instance, to reach a conversion rate of 0.3, an increase in the temperature from 370 to 850 °C leads to a reduction of the reaction time from 82.2 min to 3.7 min.

Fig. 10 presents the effect of temperature on the apparent reaction rate ( $\ln R_{\text{app}}$  versus  $1/T$ ). It highlights that the reaction of combustion can be divided into three main regimes:

- For temperatures up to 450 °C (Regime I), the intrinsic chemical reaction is slow. The concentration of oxygen can be considered as uniform inside the particle and equal to that in the bulk. The chemical reaction is the limiting step.
- For temperatures between 450 and 600 °C (Regime II), both chemical reaction and mass transport affect the rate of the combustion.
- Finally, for temperatures greater than 600 °C (Regime III), the intrinsic reactivity of the char is very high and oxygen molecule will react as soon as they have passed the boundary layer around the particle. The reaction rate is controlled by external mass transfer.

Same results were obtained for the pellet chars and Regime I was found to take place for temperatures up to 400 °C. We chose to study the reactivity of chars in Regime I. Indeed, at low combus-

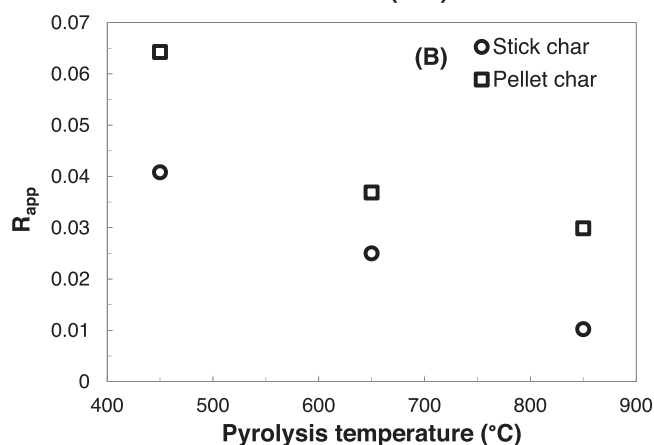
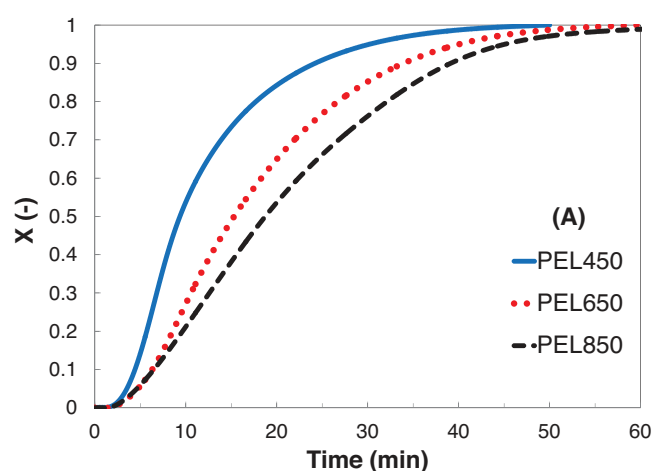


**Fig. 11.** (A) Effect of the pyrolysis temperature on the char conversion rate obtained by fast pyrolysis of beech bark pellet at 450, 650 and 850 °C. (B) Effect of the pyrolysis temperature on the apparent reactivity of char.

tion temperatures, the resistance of external transfers (heat and mass) are negligible compared to those of chemical processes and it is then possible to measure the intrinsic reactivity and kinetic of char combustion. Consequently, we took a combustion temperature of 400 °C which enables a slow chemical reaction, the absence of heat and mass transfer limitations and a better observation of the difference in reactivity for the various chars.

### 3.6.2. Effect of the pyrolysis temperature

Fig. 11(A) presents the evolution of the conversion rate versus time for the pellet chars obtained at different pyrolysis tempera-

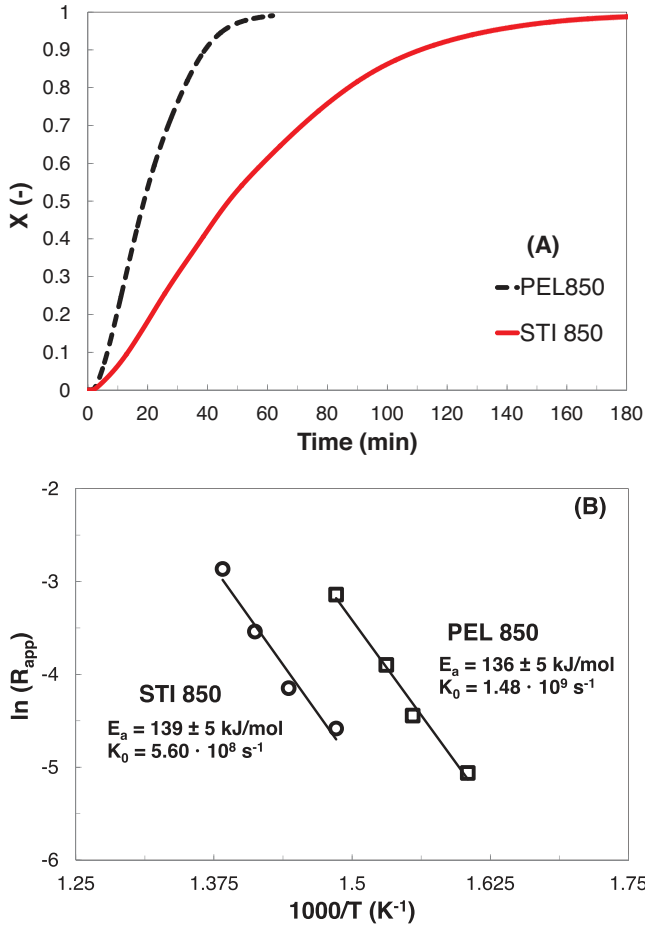


**Fig. 12.** (A) Effect of the nature of the biomass on the carbon conversion rate of char obtained by fast pyrolysis of beech bark pellet and beech stick at 850 °C, (B) Logarithm of char apparent reactivity versus  $1/T$  and kinetic parameters obtained in Regime I.

ture during the isothermal combustion in TGA at 400 °C. The char reactivity clearly decreases by increasing pyrolysis temperature. For instance, it takes 9.3 min, 15.3 min and 18.8 min to reach a conversion rate of 50% for PEL450, PEL650 and PEL850 respectively. This can be explained by the higher hydrogen and oxygen content (see Section 3.1) in the char at lower pyrolysis temperature which results in the presence of aliphatic and carbonyl groups. According to Laurendeau [3], these functionalities lead to aliphatic linkages and amorphous carbon which create cross-linking and the development of an extensive pore structure. These bonds have a weaker energy and are more susceptible to bond breakage which yields to an increase in the reactivity. At higher pyrolysis temperatures such as 850 °C, the char is more and more aromatic (see Sections 3.4 and 3.5). The aromaticity of the char leads to an ordering of the molecular structure and a decrease of the carbon edge and defect. Consequently, the amount of active sites also decreases as well as the reactivity. Fig. 11(B) shows that similar results were obtained for the stick chars, i.e. STI450, STI650 and STI850.

### 3.6.3. Effect of the initial nature of the biomass

Fig. 12 presents the effect of the biomass nature on the reactivity of char obtained by fast pyrolysis at 850 °C. We notice a strong influence of the type of biomass (beech bark pellet or beech stick). PEL850 is more reactive than STI850. For instance, according to Fig. 12(A), it takes 18.8 min and 47.0 min to reach a conversion

**Table 4**  
Pre-exponential factor and activation energy obtained from Fig. 12.

	Apparent reactivity parameter( $s^{-1}$ )	Activation energy(kJ/mol)
STI850	$K_0 = 5.60 \times 10^8$	$E_a = 139 \pm 5$
PEL850	$K_0 = 1.48 \times 10^9$	$E_a = 136 \pm 5$

rate of 50% for PEL850 and STI850, respectively. This difference in reactivity can be attributed to two different phenomena.

First, Raman and XRD analyses revealed that PEL850 and STI850 differ in their chemical structure. Stick chars have a higher amount of aromatic rings than pellet chars which are known to lower the char reactivity.

Finally, pellet chars present higher ash content than stick chars. The amount of ash may catalyze the reaction of combustion. This phenomenon can be highlighted by considering the rate of solid-state reaction as it is commonly used in the literature and presented in the following equation:

$$\frac{dX}{dt} = A \cdot \exp\left(-\frac{E_a}{RT_p}\right) \cdot P_{O_{2,s}}^n \cdot f(X) \quad (5)$$

Where  $X$  is the conversion rate,  $A$  is the pre-exponential factor ( $s^{-1} Pa^{-n}$ ),  $E_a$  is the activation energy ( $J mol^{-1}$ ),  $R$  is the gas constant ( $J mol^{-1} K^{-1}$ ),  $T_p$  is the particle temperature (K),  $P_{O_{2,s}}$  is the oxygen partial pressure at the surface of the particle (Pa) and  $n$  is the apparent reaction order which represents the char affinity with the gas reactant. This last parameter is affected by the catalytic effect of ash.  $f(X)$  is the reaction model also known as the structural factor. It corresponds to the reactive surface of the particle which depends on its size, its shape and its porosity. In the literature, this parameter is usually represented in term of conversion rate according to the following equation [45].

$$f(X) = (1 - X)^m \quad (6)$$

Where  $m$  is a geometrical reaction parameter; for example,  $m = 1$  for the Volumetric Model and  $m = 2/3$  for the Shrinking Core Model considering a spherical particle. In the following, we define an apparent reactivity parameter  $K_0$  according to the following expression:

$$K_0 = A \cdot P_{O_{2,s}}^n \cdot f(X) \quad (7)$$

Fig. 12(B) shows the evolution of char apparent reactivity  $R_{app}$  versus temperature following the Arrhenius law; linear evolution of the logarithm of  $R_{app}$  versus  $1/T$  in Regime I. From the slope and intercept of these straight lines, activation energies and parameter  $K_0$  for both STI850 and PEL850 can be determined. Their values are given in Table 4.

It can be seen that activation energies for both STI850 and PEL850 are very close to each other. Consequently, the difference in reactivity between the two chars is associated with the difference in the  $K_0$  values. For a fixed carbon conversion rate of 0.5 and a char particle diameter of 25  $\mu m$  for both chars, the structural factor  $f(X)$  is constant and the difference in  $K_0$  is attributed to the difference in the apparent reaction order “ $n$ ” and pre-exponential factor “ $A$ ”. A kinetic study was carried out on PEL850 and STI850 (not presented in this paper). It showed that the char reactivity can be well-represented by the Shrinking Core Model. Besides, pre-exponential factor was found to be higher for STI850 than PEL850. Therefore, the higher value of  $K_0$  for PEL850 is due to the difference in the apparent reaction order “ $n$ ”. Indeed, the apparent reaction order of STI850 and PEL850 was found to be 0.4 and 0.7, respectively. As this parameter is dependent on the catalytic effect of ash, it can be concluded that the higher amount of ash of PEL850 leads to a higher reactivity in combustion.

## 4. Conclusion

This paper presented the characterization of char from fast pyrolysis of biomass in fluidized bed reactor at three different pyrolysis temperatures and at atmospheric pressure. Two types of biomass were employed: beech bark pellet and beech stick.

The char is a complex solid residue with the presence of carbon, hydrogen, oxygen and inorganic matters. The chemical formula of the char is in the form of  $\text{CH}_x\text{O}_y$ . The char properties were found to be highly dependent on the pyrolysis temperature and the nature of the initial biomass. By increasing pyrolysis temperature, the main conclusions were:

- (1) Chars develop a more disordered structure with the presence of pores, vesicles and bubbles which revealed the emission of volatile products.
- (2) Hydrogen and oxygen contents as well as hydroxyl and carbonyl groups of the char decrease indicating an increase in the aromaticity and carbonaceous nature of char.
- (3) The loss of these functionalities strongly affects the oxidative reactivity of char which decreases with pyrolysis temperature.
- (4) The ratio of large to small aromatic ring system strongly increases to approach a graphitic structure but still away from graphite.

The reactivity of char was studied by isothermal combustion of char at 400 °C in TGA. The char reactivity is highly dependent on the pyrolysis temperature. At low pyrolysis temperature, the hydrogen and oxygen contents of the char led to the presence of amorphous carbon and active sites which increase the reactivity. By raising the pyrolysis temperature, the char was found to be more and more aromatic which reduces the reactivity.

Finally, the nature of the initial biomass has a significant effect on the oxidative reactivity of chars. Chars from fast pyrolysis of beech bark pellet were more reactive than chars from fast pyrolysis of beech stick. This was due to the difference in their chemical structure and ash content. Stick chars have a higher amount of aromatic rings which decreases the reactivity. Besides, a kinetic study showed that the presence of ash increases the affinity of char with oxygen and raise the reactivity.

## Acknowledgment

The authors thank the “Midi-Pyrénées Region” for financial support of this project.

## References

- [1] C. Di Blasi, Modeling chemical and physical processes of wood and biomass pyrolysis, *Prog. Energy Combust. Sci.* 34 (2008) 47–90.
- [2] A.V. Bridgwater, Review of fast pyrolysis of biomass and product upgrading, *Biomass Bioenergy* 38 (2012) 68–94.
- [3] N.M. Laurendeau, Heterogeneous kinetic of coal char gasification and combustion, *Prog. Energy Combust. Sci.* 4 (1978) 221–270.
- [4] A.V. Bridgwater, The technical and economic feasibility of biomass gasification for power generation, *Fuel* 74 (1995) 631–653.
- [5] R. Warnecke, Gasification of biomass: comparison of fixed bed and fluidized bed gasifier, *Biomass Bioenergy* 18 (2000) 489–497.
- [6] N. Mahinpey, A. Gomez, Review of gasification fundamentals and new findings: reactors, feedstock, and kinetic studies, *Chem. Eng. Sci.* 148 (2016) 14–31.
- [7] J.A. Ruiz, M.C. Juárez, M.P. Morales, P. Muñoz, M.A. Mendivil, Biomass gasification for electricity generation: review current technology barriers, *Renew. Sustain. Energy Rev.* 18 (2013) 174–183.
- [8] H. Hofbauer, R. Rauch, G. Löffler, S. Kaiser, Six years experience with the FiCfB-gasification process, *na* (2002).
- [9] P.T. Williams, S. Besler, The influence of temperature and heating rate on the slow pyrolysis of biomass, *Renew. Energy* 7 (1996) 233–250.
- [10] M. Guerrero, M.P. Ruiz, M.U. Alzueta, R. Bilbao, A. Millera, Pyrolysis of eucalyptus at different heating rates: studies of char characterization and oxidative reactivity, *J. Anal. Appl. Pyrolysis* 74 (2005) 307–314.
- [11] E. Cetin, B. Moghtaderi, R. Gupta, T.F. Wall, Influence of pyrolysis conditions on the structure and gasification reactivity of biomass char, *Fuel* 83 (2004) 2139–2150.
- [12] M. Kumar, R.C. Gupta, Influence of carbonization conditions on the gasification of acacia and eucalyptus wood chars by carbon dioxide, *Fuel* 73 (1994) 1922–1925.
- [13] C. Fushimi, K. Araki, Y. Yamaguchi, A. Tsutsumi, Effect of heating rate on steam gasification of biomass. 1. Reactivity of char, *Ind. Eng. Chem. Res.* 42 (2003) 3922–3928.
- [14] F. Mermoud, S. Salvador, L. Van de Steene, F. Golfier, Influence of the pyrolysis heating rate on the steam gasification rate of large wood char particles, *Fuel* 85 (2006) 1473–1482.
- [15] L. Lu, C. Kong, V. Sahajwalla, D. Harris, Char structural ordering during pyrolysis and combustion and its influence on char reactivity, *Fuel* 81 (2002) 1215–1225.
- [16] C. Di Blasi, G. Signorelli, C. Di Russo, G. Rea, Product distribution from pyrolysis of wood and agricultural residues, *Ind. Eng. Chem. Res.* 38 (1999) 2216–2224.
- [17] M. Garcia-Perez, X.S. Wang, J. Shen, M.J. Rhodes, F. Tian, W.J. Lee, H. Wu, C.Z. Li, Fast pyrolysis of oil mallee woody biomass: effect of temperature on the yield and quality of pyrolysis products, *Ind. Eng. Chem. Res.* 47 (2008) 1846–1854.
- [18] M. Hémati, L. El Ghezal, C. Laguerie, Etude expérimentale de la pyrolyse de sciure de bois dans un lit fluidisé de sable entre 630 et 940 °C, *Chem. Eng. J.* 42 (1989) B25–B38.
- [19] M. Asadullah, S. Zhang, Z. Min, P. Yimsiri, C.Z. Li, Effect of biomass char structure on its gasification reactivity, *Bioresour. Technol.* 101 (2010) 7935–7943.
- [20] S.Y. Zhang, J.F. Lu, J.S. Zhang, G.X. Yue, Effect of pyrolysis intensity on the reactivity of coal char, *Energy Fuels* 22 (2008) 3213–3221.
- [21] X. Zhu, C. Sheng, Evolution of the char structure of lignite under heat treatment and its influence on combustion reactivity, *Energy Fuels* 24 (2010) 152–159.
- [22] M. Zhong, S. Gao, Q. Zhou, J. Yue, F. Ma, G. Xu, Characterization of char from high temperature fluidized bed coal pyrolysis in complex atmosphere, *Particology* 25 (2016) 59–67.
- [23] R.K. Sharma, J.B. Wooten, V.L. Baliga, M.R. Hajaligol, Characterization of chars from biomass-derived materials: pectin chars, *Fuel* 80 (2001) 1825–1836.
- [24] R.K. Sharma, J.B. Wooten, V.L. Baliga, X. Lin, W.G. Chan, M.R. Hajaligol, Characterization of chars from pyrolysis of lignin, *Fuel* 83 (2004) 1469–1482.
- [25] W.S.L. Mok, M.J. Antal, Effects of pressure on biomass pyrolysis. 1. Cellulose pyrolysis products, *Thermochim. Acta* 68 (1983) 155–164.
- [26] Y. Okumura, T. Hanaoka, K. Sakanishi, Effect of pyrolysis conditions on gasification reactivity of woody biomass-derived char, *Proc. Combust. Inst.* 32 (2009) 2013–2020.
- [27] D.G. Roberts, D.J. Harris, T.F. Wall, On the effects of high pressure and heating rate during coal pyrolysis on char gasification reactivity, *Energy Fuels* 17 (2003) 887–895.
- [28] R. Zanzi, K. Sjöström, E. Björnbom, Rapid high-temperature pyrolysis of biomass in a free-fall reactor, *Fuel* 75 (1996) 545–550.
- [29] O. Senneca, P. Russo, P. Salatino, S. Masi, The relevance of thermal annealing to the evolution of coal char gasification reactivity, *Carbon* 35 (1997) 141–151.
- [30] L.B. Méndez, A.G. Borrego, M.R. Martínez-Tarazona, R. Menéndez, Influence of petrographic and mineral matter composition of coal particles on their combustion reactivity, *Fuel* 82 (2003) 1875–1882.
- [31] R.H. Hurt, A.F. Sarofim, J.P. Longwell, The role of microporous surface area in the gasification of chars from a sub-bituminous coal, *Fuel* 70 (1991) 1079–1082.
- [32] J.M. Commandré, B.R. Stanmore, S. Salvador, The high temperature reaction of carbon with nitric oxide, *Combust. Flame* 128 (2002) 211–216.
- [33] S. Salvador, J.M. Commandré, B.R. Stanmore, Reaction rates for the oxidation of highly sulphurized petroleum cokes: the influence of thermogravimetric conditions and some coke properties, *Fuel* 82 (2003) 715–720.
- [34] M. Guerrero, M. Pilar Ruiz, A. Millera, M.U. Alzueta, R. Bilbao, Characterization of biomass chars formed under different devolatilization conditions: differences between rice husk and eucalyptus, *Energy Fuels* 22 (2008) 1275–1284.
- [35] J. Szekeley, J.W. Evans, H.Y. Sohn, *Gas-solid Reactions*, Elsevier, 2012.
- [36] R. Zanzi, K. Sjöström, E. Björnbom, Rapid pyrolysis of agricultural residues at high temperature, *Biomass Bioenergy* 23 (2002) 357–366.
- [37] K.K. Pandey, A study of chemical structure of soft and hardwood and wood polymers by FTIR spectroscopy, *J. Appl. Polym. Sci.* 71 (1999) 1969–1975.
- [38] X. Colom, F. Carrillo, F. Nogués, P. Garriga, Structural analysis of photodegraded wood by means of FTIR spectroscopy, *Polym. Degrad. Stab.* 80 (2003) 543–549.
- [39] M. Zhong, S. Gao, Q. Zhou, J. Yue, F. Ma, G. Xu, Characterization of char from high temperature fluidized bed coal pyrolysis in complex atmospheres, *Particology* 25 (2016) 59–67.
- [40] D.M. Keown, X. Li, J.I. Hayashi, C.H. Li, Characterization of the structural features of char from the pyrolysis of cane trash using Fourier transform – Raman spectroscopy, *Energy Fuels* 21 (2007) 1816–1821.
- [41] D.M. Keown, X. Li, J.I. Hayashi, C.Z. Li, Evolution of biomass char structure during the oxidation in O<sub>2</sub> as revealed by FT-Raman spectroscopy, *Fuel Process. Technol.* 89 (2008) 1429–1435.
- [42] F. Tuinstra, J.L. Koenig, Raman spectrum of graphite, *J. Chem. Phys.* 63 (1970) 1126–1130.

- [43] X. Li, J.I. Hayashi, C.Z. Li, FT-Raman spectroscopic study of the evolution of char structure during the pyrolysis of a Victorian brown coal, *Fuel* 85 (2006) 1700–1707.
- [44] A. Sadezky, H. Muckenhuber, H. Grothe, R. Niessner, U. Pöschl, Raman microspectroscopy of soot and related carbonaceous materials: spectral analysis and structural information, *Carbon* 43 (2005) 1731–1742.
- [45] S. Vyazovkin, A.K. Burnham, J.M. Criado, L.A. Pérez-Maqueda, C. Popescu, N. Sbirrazzuoli, ICTAC kinetics committee recommendations for performing kinetic computations on thermal analysis data, *Thermochim. Acta* 520 (2011) 1–19.